

# Generalized Sturmians in the time-dependent frame: effect of a fullerene confining potential

Ana Laura Frapiccini<sup>1,a</sup>, Gustavo Gasaneo<sup>1</sup>, and Dario M. Mitnik<sup>2</sup>

<sup>1</sup> IFISUR, Universidad Nacional del Sur, CONICET, Departamento de Física – UNS, Av. L.N. Alem 1253, B8000CPB Bahía Blanca, Argentina

<sup>2</sup> IAFE, (UBA – CONICET), C1428EGA Buenos Aires, Argentina

Received 4 November 2016 / Received in final form 29 December 2016

Published online 16 February 2017 – © EDP Sciences, Società Italiana di Fisica, Springer-Verlag 2017

**Abstract.** In this work we present a novel implementation of the Generalized Sturmian Functions in the time-dependent frame to numerically solve the time-dependent Schrödinger equation. We study the effect of the confinement of H atom in a fullerene cage for the  $1s \rightarrow 2p$  resonant transition of the atom interacting with a finite laser pulse, calculating the population of bound states and spectral density.

## 1 Introduction

Photoionization of endohedral atoms, atoms enclosed in fullerene cages, has been the subject of intense theoretical scrutiny lately (see, e.g., [1,2] and references therein). Such systems are of interest due to the many possible applications [3–11], including drug delivery [3], quantum computation [5,6], high harmonic generation [9,10], photo-voltaics [7], and hydrogen storage [4]. Furthermore, these studies offer, from a purely theoretical standpoint, the opportunity to investigate the effects of an external environment, the fullerene, on the behavior of the enclosed atom, especially for the case of photoionization, which is of interest because small external potentials can have dramatic effects upon the structural and dynamic properties of the confined atom [1–3].

An ab-initio theoretical description of the endohedral fullerenes and their interaction with radiation demands accurate approaches that take into account electron correlations and collective modes. However, some important properties of the atoms inside a captor fullerene can be revealed by using simple semi-empirical model potentials simulating the fullerene cage. The model-potential method was a first step to study and qualitatively predict the confining effects of the cage on the spectral and dynamic properties of the atom. The external environment imposed by the fullerene cage can, in many instances, be described quite well by a simple, local, spherically symmetric, attractive cage potential that is generally taken to be of constant depth in the region of the fullerene. Photoionization of atoms which are influenced by this model potentials has been treated using a number of methodologies, such as Hartree-Fock (HF) [1,12], random-phase approximation (RPA) [1,13,14], time-dependent

close-coupling (TDCC) [15,16], R-matrix [17], and matrix iterative method [18].

In this article, we propose to use the Generalized Sturmian Functions [19] to numerically solve the time-dependent Schrödinger equation of a caged atom interacting with a laser pulse. The idea is to solve the time-dependent portion of the Schrödinger equation when the atom interacts with a pulse of finite duration, and then to effectively propagate the solution to infinite time by using the wave packet at the end of the pulse as the source term in a time-independent driven Schrödinger equation with the field-free Hamiltonian. This time-independent solution will have outgoing wave boundary conditions and all information about ionization can be extracted from it [20]. The adaptability of the Generalized Sturmian Functions is key in this methodology, since we can use exponential decaying (real) Sturmians to solve the time-dependent portion of the problem, and the outgoing wave (complex) Sturmians for the time-independent term. To propagate the time-dependent wave packet during the interaction with the pulse, we use an explicit integrating scheme known as Arnoldi [21], which is a Krylov subspace method. An extensive study of its stability and accuracy properties can be found in [22]. However, this is a new implementation of the propagation method with the Generalized Sturmian basis.

In Section 2 we present an outline of the methodology to extract the ionization amplitude and the spectral density for a one-electron atomic system. In Section 3 the numerical solution using Sturmians is outlined, for both the interaction with the pulse and the field free term. Several results analyzing the effect of the caging potential are presented in Section 4, including the study of avoided crossings due to the change in the depth of the spherical well model potential used to represent the effect

<sup>a</sup> e-mail: afrapic@uns.edu.ar

of the fullerene. We also present in this section calculations of photoionization near an avoided crossing, to study the mirror collapse of the bound states. The main results for the photoionization of the caged H atom are presented in Section 5. We compare the bare and confined H atom in the case of a (central) photon with energy 0.375 a.u., which corresponds to the  $1s \rightarrow 2p$  resonant transition of H. The parameters of the model potential represents the  $C_{36}$  and  $C_{60}$  shells, and we refer to these two cases as endo-fullerenes  $H@C_{36}$  and  $H@C_{60}$ . The results for the  $1s$  and  $2p$  bound states population during the interaction with the pulse are presented, as well as the spectral density.

Atomic units are used throughout unless otherwise indicated.

## 2 Time-dependent Schrödinger equation

We write the time-dependent Schrödinger equation (TDSE) for a two particle system interacting with an external field in the form

$$i\frac{\partial}{\partial t}\Psi(\mathbf{r}, t) = H(\mathbf{r}, t)\Psi(\mathbf{r}, t) \quad (1)$$

where the Hamiltonian can be written as

$$H(\mathbf{r}, t) = H_0 + H_{int} \quad (2)$$

with  $H_0$  the unperturbed Hamiltonian, and  $H_{int}$  the interaction with the field. The interaction with the field of an electromagnetic pulse of finite duration is

$$H_{int} = \begin{cases} f(\mathbf{r}, t) & \text{for } t_0 \leq t \leq t_{final} \\ 0 & \text{for } t > t_{final} \end{cases} \quad (3)$$

with  $\mathbf{r}$  being the electronic coordinates.

The evolution of the wave packet at  $t > t_{final}$  is equivalent to solve the time-independent Schrödinger equation given by

$$(E - H_0)\Psi_{sc}(\mathbf{r}) = \Psi(\mathbf{r}, t_{final}) \quad (4)$$

where  $H_0$  is the atomic (time-independent) Hamiltonian,  $\Psi_{sc}$  is a scattering term with outgoing boundary conditions, and  $\Psi(\mathbf{r}, t_{final})$  is the wave packet at the end of the pulse [20].

We consider now the case of one-electron atoms to show how the information for the ionization amplitude can be obtained. The atomic Hamiltonian for an atom of charge  $Z$  is

$$H_0 = T - \frac{Z}{r} \quad (5)$$

where  $T$  is the operator of the kinetic energy. At sufficiently long time after the end of the pulse, the wave packet can be written in terms of eigenstates of  $H_0$  as

$$\begin{aligned} \Psi(\mathbf{r}, t) = & \sum_n C(k_n)\psi_n(\mathbf{r})e^{-i(k_n^2/2)(t-t_{final})} \\ & + \int d\mathbf{k} C(\mathbf{k})\psi_{\mathbf{k}}^-(\mathbf{r})e^{-i(k^2/2)(t-t_{final})}, \end{aligned} \quad (6)$$

where  $\psi_{\mathbf{k}}^-$  is a momentum-normalized Coulomb wave function with incoming boundary condition and  $\psi_n$  is a bound state hydrogenic function. The coefficients  $C(k_n)$  and  $C(\mathbf{k})$  are the excitation and ionization amplitudes, respectively.

The differential probability for an electron having the energy  $E$  is determined in terms of the spectral density  $D(E, t)$ :

$$dP = D(E, t)dE, \quad (7)$$

where

$$D(E, t) = \sqrt{2E} \int |C(\mathbf{k})|^2 d\Omega_k \quad (8)$$

with  $\Omega_k$  denoting the solid angle under which the electron is emitted.

To see how to extract the coefficients  $C(\mathbf{k})$  from equation (4), we write this equation by means of the Green's function

$$\Psi_{sc}(\mathbf{r}) = \frac{1}{(E - H_0)}\Psi(\mathbf{r}', t_{final}) = G^+(\mathbf{r}, \mathbf{r}')\Psi(\mathbf{r}', t_{final}). \quad (9)$$

Using the properties of the Coulomb Green's function, we can see that the asymptotic form of the scattering function is

$$\Psi_{sc}(\mathbf{r}) \xrightarrow{r \rightarrow \infty} -\sqrt{2\pi}C(k\hat{\mathbf{r}})\frac{e^{i[kr+(Z/k)\ln 2kr]}}{r} \quad (10)$$

for an electron ejected with momentum  $k = \sqrt{2E}$ . This means that if the scattering function has the correct (outgoing wave) asymptotic behavior, the ionization amplitude can be extracted from the function at sufficiently large values of the radius  $r$ .

## 3 Numerical solution for the TDSE

### 3.1 Interaction with the pulse

To solve the TDSE equation (1) for  $t < t_{final}$  we expand the wave packet in spherical coordinates, and use generalized Sturmian Functions (GSF) [19,23]

$$\Psi(\mathbf{r}, t) = \sum_{nl} a_{nl}(t)\frac{S_{nl}(r)}{r}Y_l^0(\hat{\mathbf{r}}) \quad (11)$$

with  $a_{nl}(t)$  the expansion coefficients that depend on time and  $Y_l^m$  the spherical harmonics. The set of GSF used to solve the TDSE are real and with exponential decaying behavior at large distances.

The interaction with the pulse, within the dipole approximation, is written using the velocity gauge, and we consider here linear polarization in the  $\hat{\mathbf{z}}$  axis, thus

$$H_{int}(\mathbf{r}, t) = -i\mathbf{A}(t) \cdot \nabla_{\mathbf{r}} = -i|\mathbf{A}(t)|\frac{\partial}{\partial z} \quad (12)$$

For a photon energy  $\omega$  and a pulse of duration  $\tau$  we write

$$|\mathbf{A}(t)| = A_0g(\omega, t)\sin(\omega t) \quad \text{for } t \in [0, \tau]. \quad (13)$$

Substituting the expansion (11) into the Schrödinger equation (1) and projecting onto the basis set, we obtain a matrix equation on the form

$$i\mathbf{B}\frac{\partial}{\partial t}\mathbf{a}(t) = \mathbf{H}(t)\mathbf{a}(t) \quad (14)$$

with  $\mathbf{B}$  the overlap matrix,  $\mathbf{H}$  the matrix representation of the Hamiltonian and  $\mathbf{a}(t)$  the time-dependent coefficients vector. Since the GSF set used has exponential decay, the one-dimensional radial integrals involving the calculation of the overlap and Hamiltonian matrices can be performed up to a finite radius. For this computation we use a Gauss-Legendre quadrature.

While the overlap and atomic Hamiltonian matrices are diagonal with respect to the electronic angular momentum  $l$ , the term  $H_{int}$  couples the angular momenta for  $l' = l \pm 1$ . The total dimension of the matrices will depend on the number of GSF used in the expansion in equation (11). If we call  $N_{max}$  the maximum number for the radial index  $n$  and  $l_{max}$  the maximum angular momenta included, then the matrices in equation (14) have dimension  $N_{tot} \times N_{tot}$  with  $N_{tot} = N_{max} \times l_{max}$ .

To perform the time propagation up to  $t = \tau$  we use a Krylov subspace method usually called Arnoldi algorithm [21]. The choice of the propagator is not trivial, and it was based on a previous extensive work analyzing the performance of several explicit and implicit algorithms [22]. The implicit scheme was a predictor-corrector with a fully implicit four-stage Radau IIA method of order 7 as a corrector, and an adapted time step. Although highly accurate, the computer time to perform the propagation of the TDSE with this algorithm is longer compared with the explicit schemes. We concluded that since we were seeking for a precision in the energy spectrum of  $\approx 10^{-8}$ , Arnoldi propagator was the better choice for our problem.

A detailed study of this method can be found in [22], here we briefly recall the main features of this propagating scheme. In this case, we use Cholesky decomposition of the overlap matrix to form an orthonormal basis, so equation (14) now reads

$$\frac{\partial}{\partial t}\mathbf{b}(t) = -i\hat{\mathbf{H}}(t)\mathbf{b}(t), \quad (15)$$

where  $\mathbf{B} = \mathbf{U}^\dagger\mathbf{U}$ , the new coefficients  $\mathbf{b} = \mathbf{U}\mathbf{a}$  and  $\hat{\mathbf{H}} = (\mathbf{U}^\dagger)^{-1}\mathbf{H}\mathbf{U}^{-1}$ .

If we assume that the time interval is sufficiently small that the Hamiltonian may be treated as constant in time over a time step  $\delta t$ , it is trivial to demonstrate that equation (15) has a solution given by

$$\mathbf{b}(t + \delta t) = e^{-i\hat{\mathbf{H}}(t)\delta t}\mathbf{b}(t). \quad (16)$$

Instead of performing the full diagonalization of the matrix  $\hat{\mathbf{H}}(t)$  to solve the exponential, we can define a subset of linearly independent vectors

$$K_{m+1} = \text{span}\{\mathbf{b}, \hat{\mathbf{H}}\mathbf{b}, \dots, \hat{\mathbf{H}}^m\mathbf{b}\}. \quad (17)$$

which form the Krylov subspace. Then we use Gram-Schmidt orthogonalization successively to form an orthonormal basis  $Q_{m+1} = \{\mathbf{q}_0, \dots, \mathbf{q}_m\}$  with  $\mathbf{q}_0 = \mathbf{b}/|\mathbf{b}|$ , and the  $\mathbf{q}_k$  are obtained by calculating  $\hat{\mathbf{H}}\mathbf{q}_{k-1}$  and then orthonormalizing each vector with respect to  $\mathbf{q}_0, \dots, \mathbf{q}_{k-1}$ . If we define  $\mathbf{Q}$  to be a matrix formed by the  $m+1$  column vectors  $\mathbf{q}_k$ , we can write

$$\hat{\mathbf{H}}\mathbf{Q} = \mathbf{Q}\mathbf{h}, \quad (18)$$

giving

$$\mathbf{h} = \mathbf{Q}^\dagger\hat{\mathbf{H}}\mathbf{Q}. \quad (19)$$

We see here that  $\mathbf{h}$  is the Krylov subspace representation of the full Hamiltonian  $\hat{\mathbf{H}}$ , and that in this procedure, we obtain simultaneously the Krylov vectors  $\mathbf{q}_0, \dots, \mathbf{q}_m$ . For non-Hermitian matrices, the method reduces the dense matrix  $\mathbf{h}$  to an upper Hessenberg form, and in the particular case of Hermitian matrices, to a symmetric tridiagonal form. Once we obtain the orthonormal Krylov subspace  $\mathbf{Q}$  and the representation  $\mathbf{h}$  of the Hamiltonian, it can be easily shown that equation (16) can be written as

$$\chi(t + \delta t) = \mathbf{Q}e^{-i\mathbf{h}\delta t}\mathbf{Q}^\dagger\chi(t). \quad (20)$$

Typical sizes of the matrix  $\mathbf{h}$  for one-dimensional problem go from 10 to less than 100, so the computational work involving the diagonalization of the matrix is much less than in the case of the full Hamiltonian. The rest of the scheme involves only matrix-vector and scalar products, which makes it very efficient regarding the time of the calculations.

All the matrix operations involved in the algorithm (such as Cholesky decomposition, matrix-vector products and linear system equation solvers) were calculated using LAPACK [24] subroutines.

### 3.2 Scattering term

Once the propagation of the wave-packet until the end of the pulse is performed, we have to solve equation (4) to find the scattering term. We use a similar expansion to that of the wave packet

$$\Psi_{sc}(\mathbf{r}) = \sum_{nl} c_{nl}^+ \frac{S_{nl}^+(r)}{r} Y_l^0(\hat{\mathbf{r}}) \quad (21)$$

where the + stress the fact that the GSF now have outgoing wave behavior, and are complex. Replacing this expansion in equation (4) and projecting onto the basis set we have

$$(\mathbf{E}\mathbf{B} - \mathbf{H}_0)\mathbf{c}^+ = \tilde{\mathbf{a}}(t_{final}) \quad (22)$$

with  $\mathbf{B}$  and  $\mathbf{H}_0$  the overlap and atomic Hamiltonian matrices for the outgoing GSF,  $\mathbf{c}^+$  the coefficient vector and

$$\tilde{\mathbf{a}}_{n'l'}(t_{final}) = \sum_{nl} a_{nl}(t_{final}) \langle S_{n'l'}^+ | S_{nl} \rangle \delta_{l'l}. \quad (23)$$

The one-dimensional radial integrals involving the calculation of  $\mathbf{H}_0$  and  $\tilde{\mathbf{a}}(t_{final})$  have all finite range,

and can be calculated easily by means of the Gauss-Legendre quadrature. For the overlap integral, however, the GSF are defined in all radial space, and a finite quadrature is not suitable. If we do not take into account the external part of the overlap integrals the evaluation can be interpreted as a box-based-type calculation. The complete calculation is performed by using the asymptotic forms of the GSF, and the inner (finite) term is solved using a Gauss-Legendre quadrature. Details on this numerical aspects can be found in [25].

From equation (11) then we can extract the information on the ionization amplitude, using the asymptotic form of the GSF

$$S_{nl}^+(r) \xrightarrow{r \rightarrow \infty} e^{i[kr + (Z/k) \ln 2kr]} \quad (24)$$

and combining this with the expansion in equation (21) we have

$$C(k\hat{\mathbf{r}}) = -\frac{1}{\sqrt{2\pi}} \sum_{nl} c_{nl}^+ Y_l^0(\hat{\mathbf{r}}), \quad (25)$$

the dependence in  $k$  is in the coefficients  $c_{nl}^+$ .

## 4 Effects of the fullerene shell on the bound states of H

### 4.1 Avoided crossing and mirror collapse

In this section we briefly analyze the effect of the confinement of the H atom in a fullerene modeled by a spherical well

$$V_w(r) = \begin{cases} -U_0 & \text{if } r_c \leq r \leq r_c + \Delta \\ 0 & \text{otherwise} \end{cases} \quad (26)$$

where  $r_c$  is the inner radius of the well and  $\Delta$  its thickness. This potential was already implemented with the GSF in a previous work to study the ‘mirror collapse’ effects in an S-wave model of Helium [26].

The bound states of the caged atom are obtained by solving the time-independent Schrödinger equation (TISE)

$$[H_0 + V_w] \Psi_\nu(\mathbf{r}) = E_\nu \Psi_\nu(\mathbf{r}) \quad (27)$$

with  $H_0$  as in equation (5) and expanding the wave function with real, exponential decaying GSF

$$\Psi_\nu(\mathbf{r}) = \sum_{nlm} a_{nl} \frac{S_{nl}(r)}{r} Y_l^m(\hat{\mathbf{r}}). \quad (28)$$

The generalized eigenvalue problem to solve is

$$[\mathbf{H}_0 + \mathbf{V}_w] \mathbf{a}_{\nu,l} = E_{\nu,l} \mathbf{B} \mathbf{a}_{\nu,l} \quad (29)$$

for each angular momentum  $l$  and  $m = 0$ . All matrices are real and symmetric, and the overlap term is also positive definite. The size of the matrices depend on the number  $N_{max}$  of GSF in the expansion (28), so the dimension of the matrices will be  $N_{max} \times N_{max}$ . In all the calculations shown in this section, we used a value of  $N_{max} = 120$  for each value of  $l$ .

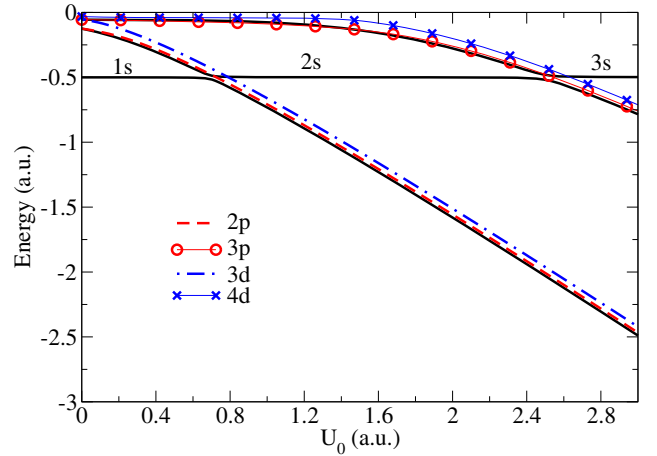


**Fig. 1.** Energies of the H atom confined in a spherical well with  $r_c = 5.75$  a.u. and  $\Delta = 1.89$  a.u. as a function of  $U_0$ .

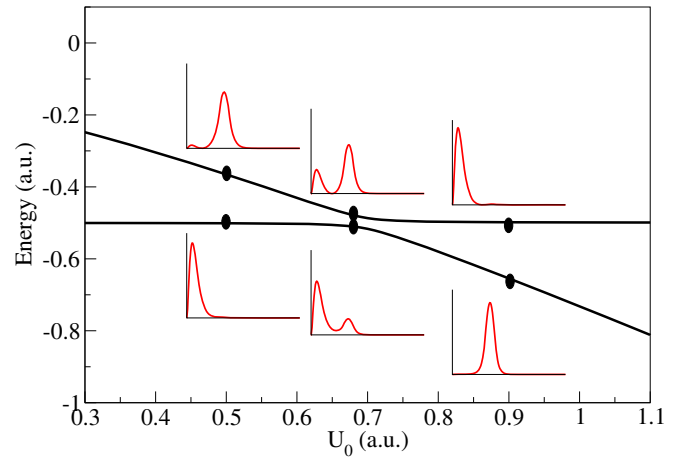


**Fig. 2.** Radial probability density for the 1s (down) and 2s (up) states near a crossing.

For this study, we fix the values of  $r_c$  and  $\Delta$  and calculate the eigenvalues for  $U_0$  in a range from 0 to 3 a.u. We use the data provided by Xu et al. [27] for a fullerene molecule  $C_{60}$ , which is  $r_c = 5.75$  a.u. and  $\Delta = 1.89$  a.u. In Figure 1 we show the results for the first bound states, from 1s to 4d energy levels. We can see here how, for low values of  $U_0$ , the 1s energy remains constant, so it does not feel the presence of the well. This is because the 1s state is mostly confined near the origin, and far from the inner wall of the potential. This is not the same for the 2s state, which has a higher probability to be inside the well, so the energy lowers as  $U_0$  increases. When the depth of the well is approximately 0.7 the 1s and 2s energies are very similar, there is strong interaction between the two states and the wave functions are mixed, leading to the avoided crossing seen in Figure 1.

In Figure 2 we can see the radial probability density  $\int r^2 |\Psi_\nu(\mathbf{r})|^2 d\Omega_r$  for the 1s and 2s states in the vicinity of the avoided crossing. It is seen how for low values of  $U_0$  the 1s level is bound in the inner well, while the 2s is confined mostly inside the well. For the case of  $U_0 = 0.7$ , the 2s state bound in this well has energy comparable

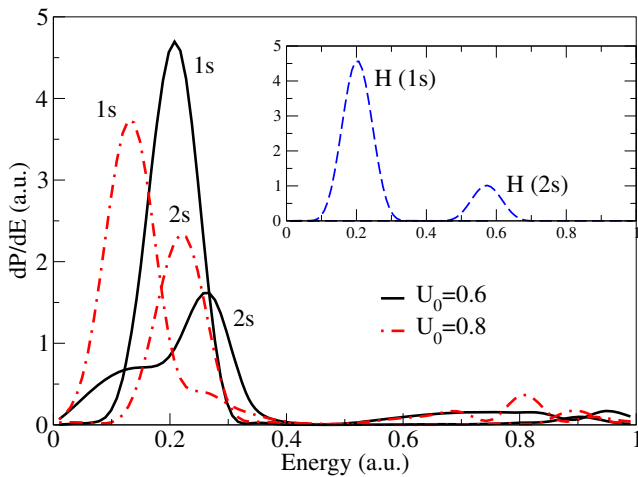


**Fig. 3.** Ejected electron spectrum from the 1s and 2s states of H confined in two different potential wells. The pulse has peak intensity  $10^{15}$  W/cm<sup>2</sup>, photon energy  $\omega = 0.7$  a.u. and 10 optical cycles, which gives  $\tau \approx 90$  a.u. of pulse duration. The inset shows photoionization of the bare H atom from 1s and 2s states.

with the 1s state, the probability density of both levels being very similar, with the electron bound either to the inner well or inside the well. As the value of  $U_0$  increases, since the lowest energy level corresponds to the 1s, the level now bound in the outer well is the 1s, whereas the level in the inner well is the 2s. This phenomenon, in which the 2s ‘collapses’ into the inner well, while the 1s, formerly in the inner well, simultaneously ‘collapses’ into the outer well, is referred to as ‘mirror collapse’. This behavior is repeated for the 2s and 3s energy levels close to  $U_0 = 2.5$ , and for further  $s$  levels for higher values of  $U_0$ . The results obtained with the GSF are in accordance with those calculated by Connerade et al. [28].

#### 4.2 Photoionization near an avoided crossing

We complete the study of the ‘mirror collapse’ of the 1s and 2s bound states around  $U_0 \approx 0.7$  by calculating the photoionization of this confined atoms, using the methodology described in Section 3. The interaction with the pulse is as described in equation (13) with a sine square envelope  $g(\omega, t) = \sin\left(\frac{\pi}{\tau}t\right)^2$  with a total duration of  $\tau = 2\pi n_c/\omega$ , where  $n_c$  is an integer giving the number of optical cycles.

We consider photoionization from initial state 1s and 2s for the H atom confined in the potential well with depth  $U_0 = 0.6$  and  $U_0 = 0.8$ , with  $r_c$  and  $\Delta$  fixed as in the avoided crossing calculations.

All the calculations shown in this section were performed using  $N_{max} = 120$  and  $l_{max} = 5$ , and the size of the Krylov space was  $n_{Krylov} = 15$ , with a fixed time step of  $\delta t = 0.03$ .

Figure 3 shows how the spectrum reflects the ‘collapse’ of the 1s into the 2s bound state, since the photoionization spectrum from the 1s state for  $U_0 = 0.6$  is similar

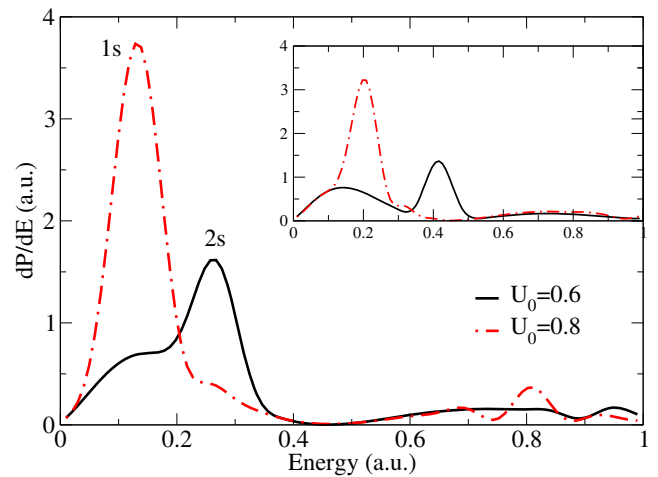


**Fig. 4.** Ejected electron spectrum from the 2s for  $U_0 = 0.6$  and 1s for  $U_0 = 0.8$  states of H confined (same as Fig. 3) compared with the photoionization of the bare well (no Coulomb interaction) from 1s states (shown in the inset). The data for the pulse is the same as in Figure 3.

to the one for the 2s with  $U_0 = 0.8$ . Both these cases are similar to the photoionization of the bare H atom, in which the main process consist of the emission of  $p$  electrons after absorbing a photon of  $\omega = 0.7$  from the 1s or 2s state. However, when the initial state are either the 2s for  $U_0 = 0.6$  or the 1s for  $U_0 = 0.8$ , the electron is confined mostly inside the well (see Fig. 2), and the spectrum resembles that of the bare spherical well (without Coulomb interaction), as seen in Figure 4.

### 5 Study of the 1s-2p resonance

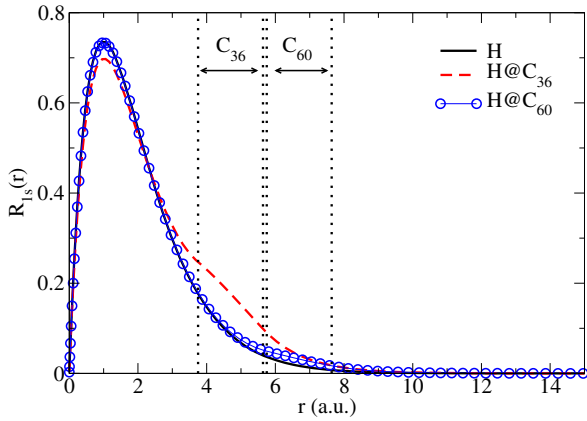
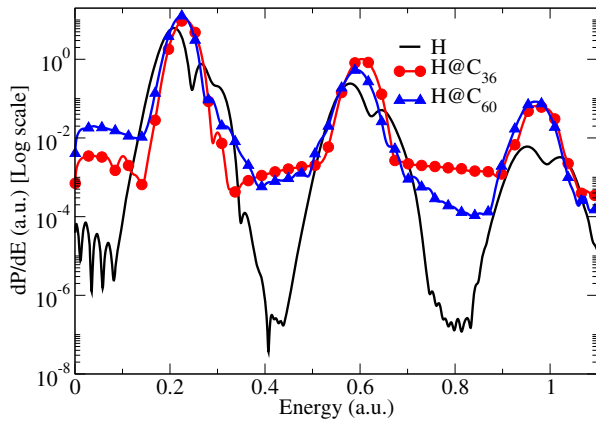
The model potential in equation (26) has been already used in studies of confinement resonances in the photoionization cross section [18,29]. In this section we study the effects of the confinement of the H atom in a C<sub>36</sub> or C<sub>60</sub> cage, compared with the bare atom, for the photoionization with an intense pulse of  $\omega = 0.375$  a.u. Since this photon energy corresponds to the 1s–2p transition frequency in H, we expect Rabi oscillations to manifest in the evolution of the population of the bound states. We want to explore if this oscillations in the population remain once the atom is confined in the C cage.

The interaction with the pulse is the same as previous calculations, a sine square envelope  $g(\omega, t) = \sin\left(\frac{\pi}{\tau}t\right)^2$  with a total duration of  $\tau = 2\pi n_c/\omega$ . In all the calculations presented now the peak intensity  $5 \times 10^{14}$  W/cm<sup>2</sup> and 16 optical cycles, which gives  $\tau \approx 268$  a.u. of pulse duration. The number of cycles was chosen so the pulse is long enough to see a few Rabi oscillations, but not extremely demanding on the computational level. For the C<sub>60</sub> cage, we use the parameters of the model potential found in [27,30]:  $U_0 = 8.22$  eV,  $r_c = 5.75$  a.u. and  $\Delta = 1.89$  a.u., and for the C<sub>36</sub> [18]:  $U_0 = 8.68$  eV,  $r_c = 3.75$  a.u. and  $\Delta = 1.89$  a.u.

All the calculations shown in this section were performed using  $N_{max} = 300$  and  $l_{max} = 15$ , and the size

**Table 1.** Lowest energies of the bound states of the bare H and caged H atom in atomic units.

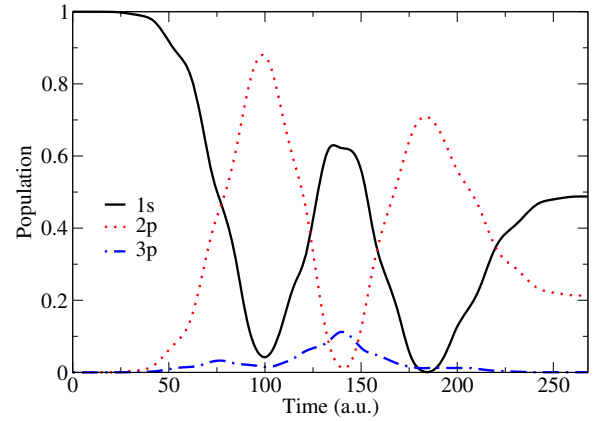
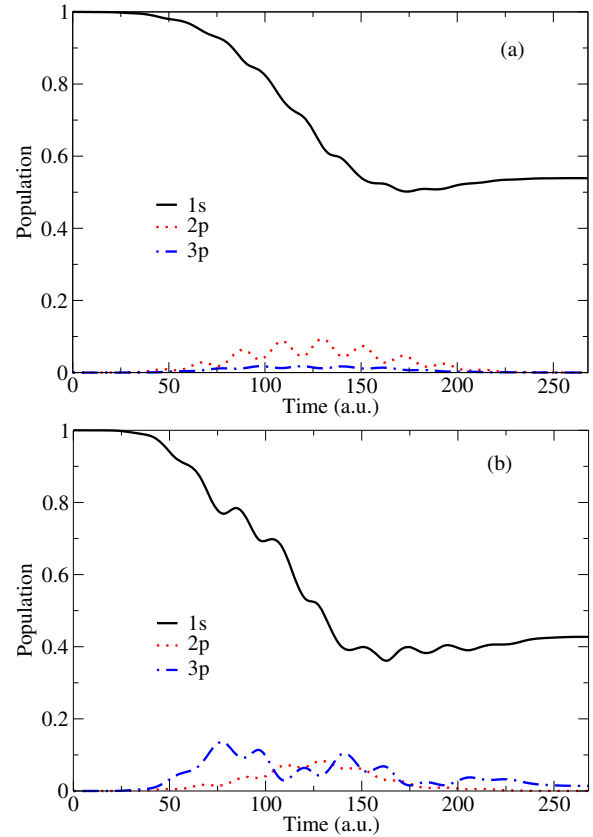
State	H	H@C <sub>36</sub>	H@C <sub>60</sub>
1s	-0.50000	-0.51098	-0.50038
2s	-0.12500	-0.27605	-0.27605
2p	-0.12500	-0.27309	-0.23103
3p	-0.0555	-0.06060	-0.06176

**Fig. 5.** Radial part of the ground state wave function for the caged and bare H atom.**Fig. 6.** Ejected electron spectrum of the bare and caged H atom for a pulse with sine square envelope,  $5 \times 10^{14}$  W/cm<sup>2</sup> peak intensity, 16 optical cycles and  $\omega = 0.375$  a.u. of photon energy.

of the Krylov space was  $n_{Krylov} = 60$ , with a fixed time step of  $\delta t = 0.03$ .

In Table 1 we show the energies of the lowest bound states for the three endofullerenes to study and the bare H atom. We can see in Figure 5 that while the 1s ground state function is hardly modified by the presence of the C<sub>60</sub> cage, the C<sub>36</sub> cage is located closer to the main maximum, and the electron has a higher probability of being trapped inside the cage.

The results for the ejected electron energy spectrum are shown in Figure 6. We can see here the splitting of the ATI peaks corresponding to the Autler-Townes doublet [31], which originates from ionization of the 2p state resonantly coupled to the 1s state. This coupling (Rabi

**Fig. 7.** Population of the 1s, 2p and 3p energy states of H during the interaction with the pulse with  $5 \times 10^{14}$  W/cm<sup>2</sup> peak intensity, 16 optical cycles and  $\omega = 0.375$  a.u. of photon energy.**Fig. 8.** Population of the 1s, 2p and 3p energy states of H@C<sub>36</sub> (a) and H@C<sub>60</sub> (b) during the interaction with the pulse with  $5 \times 10^{14}$  W/cm<sup>2</sup> peak intensity, 16 optical cycles and  $\omega = 0.375$  a.u. of photon energy.

oscillations) can be seen in Figure 7, where it is shown that the 3p state is also populated during the pulse. In the case of the caged H atom, we show in Figure 8 how the coupling between the 1s and 2p state disappears. The photon energy is enough to excite the electron in the ground state to the 2p state, and the 3p state is also populated

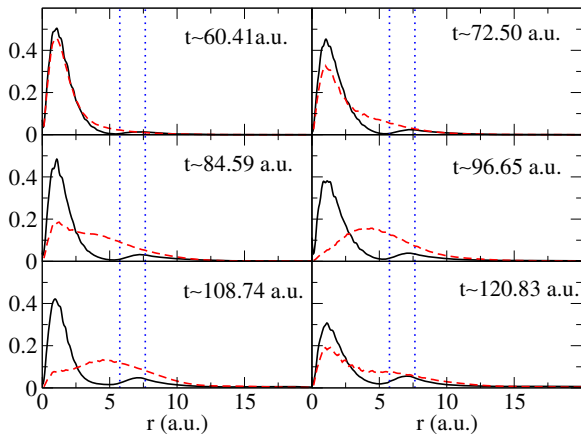


**Fig. 9.** Radial probability density of the wave packet of H@C<sub>60</sub> (full line) and H (broken line) interacting with the pulse at several stages of time. The dotted vertical line shows the location of the C<sub>60</sub> cage.

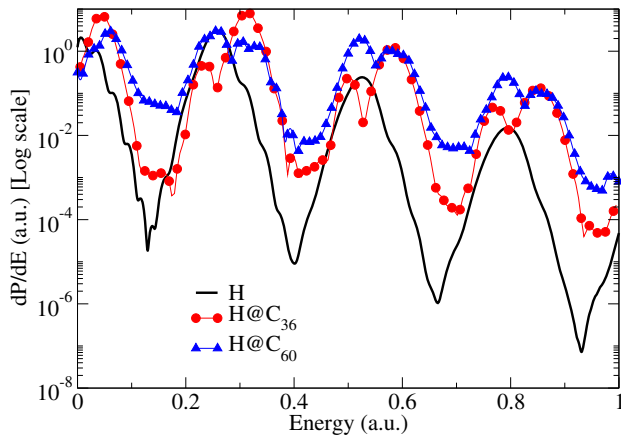


**Fig. 10.** Ejected electron spectrum of the bare and caged H atom for a pulse with sine square envelope,  $5 \times 10^{14}$  W/cm<sup>2</sup> peak intensity, 16 optical cycles and  $\omega = 0.27$  a.u. of photon energy.

in both confined atoms. Figure 9 shows the time evolution of radial probability of the wave packet for the H@C<sub>60</sub> and H atom. Here we can see that for the endohedral atom the electron can ‘move’ from the 1s to a p state inside the cage, and in this case it remains in the outer wall of the well, before being ejected to the continuum. Compared to the evolution of the H atom at the same times, we see that the electron performs a Rabi oscillation between the 1s and 2p states. For the H@C<sub>36</sub> a similar process is observed, but since the 1s ground state (see Fig. 5) can be inside the cage, the radial probability is more evenly distributed inside the well.

We also performed calculations for a photon energy of  $\omega = 0.27$  a.u., which we can see from Table 1 is approximately the energy required for the 1s–2p transition for the H@C<sub>60</sub> fullerene. In Figure 10 we show the ejected electron energy spectrum. We see here that for the bare H atom, the spectrum shows the ATI peaks with no splitting, since the photon energy is not enough to couple the

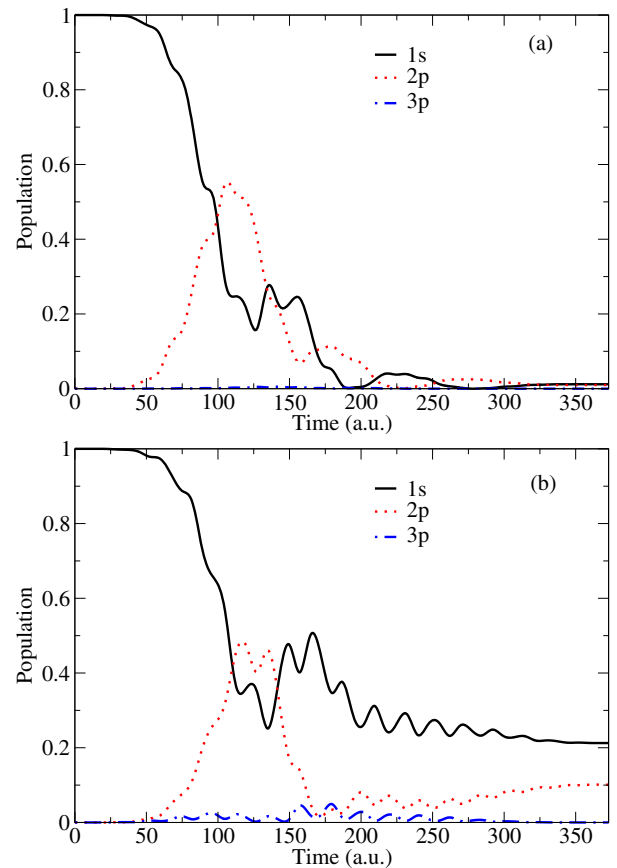


**Fig. 11.** Population of the 1s, 2p and 3p energy states of H@C<sub>36</sub> (a) and H@C<sub>60</sub> (b) during the interaction with the pulse with  $5 \times 10^{14}$  W/cm<sup>2</sup> peak intensity, 16 optical cycles and  $\omega = 0.375$  a.u. of photon energy.

1s and 2p states. However, for the caged atoms, the first peak shows no splitting, whereas the other ones do.

Figure 11 shows the population of states during the interaction with the pulse for the caged atoms. In these cases, the coupling between the 1s and 2p states does not disappear completely, and one oscillation is almost performed.

## 6 Conclusions

In this contribution, we develop an ab-initio methodology to solve the time-dependent Schrödinger equation of an atom interacting with an electromagnetic pulse of finite duration. The approach is based on the Generalized Sturmian Functions, and their adaptability to define different asymptotic behaviors. We show that with this basis set, we can solve the time-dependent Schrödinger equation, and then transform the problem in a linear equation with a scattering term to extract the information about the ionization process. This method presents the advantage of not performing integrals to obtain the ionization amplitude and the energy spectrum, since we can define the GSF to have outgoing asymptotic behavior.

We present an application by studying the influence of the confinement of the H atom in a fullerene cage  $C_{36}$  and  $C_{60}$ . We perform a brief study of the avoided crossing with a simple spherical well potential to represent the fullerene. We observe the degeneracies in energy around the points denoted as crossings, which become more evident when studying the photoionization near said points. In the particular case shown, the collapse of the  $1s$  and  $2s$  bound states is reflected in the energy spectrum, since it becomes more like the spectrum of the bare H atom or the bare well before or after the crossing.

Finally, we calculated the ionization of the bare H and caged atom interacting with a strong, short pulse in the resonant  $1s \rightarrow 2p$  frequency for H and  $H@C_{60}$ . For the  $\omega = 0.375$  a.u. case, we observed the coupling of the  $1s$  and  $2p$  in the population of the bound states during the interaction with the pulse for the bare H atom, while in the presence of the cages the coupling disappears. This is also reflected in the energy spectrum, where for the H atom there is a splitting of the peaks which is not present in the caged atoms. For  $\omega = 0.27$  a.u., the resonant frequency for  $H@C_{60}$ , the population of the caged atoms shows that the coupling does not disappear completely, and while the first peak in the energy spectrum is not split, the subsequent peaks present a splitting.

The methodology presented proved to be a useful approach to solve the TDSE avoiding the use of integrals to obtain ionization amplitudes. Although for the case of the H and caged atoms the asymptotic solution is known, this technique can be extended to two-electron atom targets, or different one particle problems where the asymptotic condition is not analytical.

We acknowledge the support by Grant No. PIP 201301/607 CONICET (Argentina) also thank the support by Grant No. PGI (24/F059) of the Universidad Nacional del Sur.

## References

- V.K. Dolmatov, *Photoionization of Atoms Encaged in Spherical Fullerenes*, Vol. 58 of *Advances in Quantum Chemistry* (Academic Press, 2009)
- V.K. Dolmatov, A.S. Baltentkov, J.P. Connerade, S.T. Manson, *Radiat. Phys. Chem.* **70**, 417 (2004)
- J.P. Connerade, *The Fourth International Symposium "Atomic Cluster Collisions: Structure and Dynamics from the Nuclear to the Biological Scale" (ISACC 2009)*, Vol. 1157 of *AIP Conference Proceedings* (2009)
- Y. Zhao, Y.H. Kim, A.C. Dillon, M.J. Heben, S.B. Zhang, *Phys. Rev. Lett.* **94**, 155504 (2005)
- C. Ju, D. Suter, J. Du, *Phys. Rev. A* **75**, 012318 (2007)
- W. Harneit, K. Huebener, B. Naydenov, S. Schaefer, M. Scheloske, *Phys. Status Solidi B* **244**, 3879 (2007)
- R.B. Ross, C.M. Cardona, D.M. Guldi, S.G. Sankaranarayanan, M.O. Reese, N. Kopidakis, J. Peet, B. Walker, G.C. Bazan, E.E.A. van Keuren, *Nat. Mater.* **8**, 208 (2009)
- A. Stróżecka, K. Muthukumar, A. Dybek, T.J. Dennis, J.A. Larsson, J. Mysliveček, B. Voigtländer, *Appl. Phys. Lett.* **95**, 133118 (2009)
- R. Hatakeyama, Y.F. Li, T.Y. Kato, T. Kaneko, *Appl. Phys. Lett.* **97**, 013104 (2010)
- G.P. Zhang, D.A. Strubbe, S.G. Louie, T.F. George, *Phys. Rev. A* **84**, 023837 (2011)
- P.V. Redkin, M.B. Danailov, R.A. Ganeev, *Phys. Rev. A* **84**, 013407 (2011)
- V.K. Dolmatov, S.T. Manson, *Phys. Rev. A* **73**, 013201 (2006)
- M.Y. Amusia, A.S. Baltentkov, U. Becker, *Phys. Rev. A* **62**, 012701 (2000)
- M.Y. Amusia, A.S. Baltentkov, *Phys. Rev. A* **73**, 062723 (2006)
- J.A. Ludlow, T.G. Lee, M.S. Pindzola, *Phys. Rev. A* **81**, 023407 (2010)
- T. Lee, J.A. Ludlow, M.S. Pindzola, *J. Phys. B* **45**, 135202 (2012)
- T.W. Gorczyca, M.F. Hasoglu, S.T. Manson, *Phys. Rev. A* **86**, 033204 (2012)
- A.N. Grum-Grzhimailo, E.V. Gryzlova, S.I. Strakhova, *J. Phys. B* **44**, 235005 (2011)
- G. Gasaneo, L.U. Ancarani, D.M. Mitnik, J.M. Randazzo, A.L. Frapiccini, F.D. Colavecchia, *Proceedings of MEST 2012: Exponential Type Orbitals for Molecular Electronic Structure Theory*, Vol. 67 of *Advances in Quantum Chemistry* (Academic Press, 2013)
- A. Palacios, C.W. McCurdy, T.N. Rescigno, *Phys. Rev. A* **76**, 043420 (2007)
- Y. Saad, *SIAM J. Numer. Anal.* **29**, 209 (1992)
- A.L. Frapiccini, A. Hamido, S. Schröter, D. Pyke, F. Mota-Furtado, P.F. O'Mahony, J. Madronero, J. Eiglsperger, B. Piraux, *Phys. Rev. A* **89**, 023418 (2014)
- A.L. Frapiccini, V.Y. Gonzalez, J.M. Randazzo, F.D. Colavecchia, G. Gasaneo, *Int. J. Quantum Chem.* **107**, 832 (2007)
- E. Anderson, Z. Bai, C. Bischof, S. Blackford, J. Demmel, J. Dongarra, J. Du Croz, A. Greenbaum, S. Hammarling, A. McKenney, D. Sorensen, *LAPACK Users' Guide*, 3rd edn. (Society for Industrial and Applied Mathematics, Philadelphia, PA, 1999)
- J.M. Randazzo, F. Buezas, A.L. Frapiccini, F.D. Colavecchia, G. Gasaneo, *Phys. Rev. A* **84**, 052715 (2011)
- D.M. Mitnik, J. Randazzo, G. Gasaneo, *Phys. Rev. A* **78**, 062501 (2008)
- Y.B. Xu, M.Q. Tan, U. Becker, *Phys. Rev. Lett.* **76**, 3538 (1996)
- J.P. Connerade, V.K. Dolmatov, P.A. Lakshmi, S.T. Manson, *J. Phys. B* **32**, L239 (1999)
- A.S. Baltentkov, U. Becker, S.T. Manson, A.Z. Msezane, *J. Phys. B* **43**, 115102 (2010)
- J.P. Connerade, A.V. Solov'yov, *J. Phys. B* **38**, 807 (2005)
- S. Autler, C. Townes, *Phys. Rev.* **100**, 703 (1955)